

# Prospects for Measurements of Rare $B$ Decays and Other Heavy Flavour Physics at CMS

K. A. Ulmer<sup>a</sup>

on behalf of the CMS Collaboration

<sup>a</sup>Department of Physics, University of Colorado, Boulder, CO 80309

The Compact Muon Solenoid (CMS) is a multi-purpose detector operating at the Large Hadron Collider at CERN. Its excellent tracking system, combined with low momentum muon trigger capabilities, allows for precise studies of heavy flavour physics. The capabilities of the CMS experiment in this field have been studied in several benchmark processes. These studies are based on a full detector simulation and show the capability of CMS to identify, select and reconstruct heavy flavour decays, which present a significant challenge due to the high backgrounds and relatively low particle momenta. After a description of the detector, the trigger system, and the trigger strategy for  $B$  physics, four heavy flavour analyses in CMS are presented: exclusive  $B_s^0$  decays to  $J/\psi\phi$  and to  $\mu^+\mu^-$ ; a study of the  $B_c^+$  meson; and the decay  $\tau^- \rightarrow \mu^-\mu^-\mu^+$ .

Presented at *BEACH 2008: The 8th International Conference on Hyperons, Charm, and Beauty Hadrons*, Columbia, South Carolina, USA June 23rd 2008.

## 1. INTRODUCTION

The Compact Muon Solenoid (CMS) is one of two general purpose experiments built to collect data at the Large Hadron Collider (LHC) at CERN beginning in Fall 2008. The LHC is a proton-proton collider designed to operate at a center-of-mass energy of 14 TeV opening a new energy frontier to the world of particle physics. The CMS detector will explore the full range of physics possible at the LHC including a varied heavy flavour programme.

The LHC is designed to operate at an instantaneous luminosity of  $10^{34} \text{ cm}^{-2} \text{ s}^{-1}$ , with an integrated luminosity of  $\sim 100 \text{ fb}^{-1}/\text{year}$ . It is foreseen that ramping up to full luminosity will take several years. It is during these initial “low luminosity” years, with instantaneous luminosities up to  $2 \times 10^{33} \text{ cm}^{-2} \text{ s}^{-1}$ , that the prospects for heavy flavour physics are the most promising at CMS.

The total  $b\bar{b}$  production cross section at the LHC is expected to be  $\sim 500 \mu\text{b}$ , which is  $\sim 10$  times larger than at the Tevatron and will provide a sample of  $5 \times 10^{11} b\bar{b}/\text{fb}^{-1}$ . The  $b\bar{b}$  cross section,

however, is small compared to the total  $pp$  cross section so measuring  $b$ -flavoured hadrons requires sorting through large backgrounds. At the design luminosity it becomes nearly impossible to trigger efficiently on the low  $p_T$  dimuon events used to identify many of the heavy flavour physics signals possible at CMS due to trigger bandwidth. Most of the  $B$  physics programme at CMS will be performed in the initial years of running at the LHC when the luminosity is lower.

In these proceedings the prospects for measurements from CMS for four benchmark processes are considered: a search for new physics in the branching fraction of  $B_s^0 \rightarrow \mu^+\mu^-$ ; a study of  $B_s^0$  mixing and  $CP$  violation in  $B_s^0 \rightarrow J/\psi\phi$ ; a study of the  $B_c^+$  meson properties reconstructed in the channel  $B_c^+ \rightarrow J/\psi\pi^+$ ; and a search for lepton flavour violation (LFV) in the decay  $\tau^- \rightarrow \mu^-\mu^-\mu^+$ .

## 2. THE CMS DETECTOR

The CMS detector is described in detail elsewhere [1]. The detector components most relevant for heavy flavour physics are the tracking

system and the muon detectors described below.

The CMS tracking system is located, along with electromagnetic and hadronic calorimeters, inside a superconducting solenoid that generates a 3.8 T field. At design luminosity, 10-20 minimum bias interactions are expected per bunch crossing producing approximately 1000 reconstructible tracks in the tracker. The dense tracking environment requires good spatial resolution and high efficiency over a large momentum range. The resolution on the transverse momentum is required to be  $\sim 1\%$  at a track momentum of 1 GeV to be able to reconstruct narrow resonances, and good impact parameter resolutions are needed to reconstruct secondary vertices. The CMS tracker is an all-silicon design with mid-rapidity charged particles tracked by three layers of silicon pixel detectors, made of 66 million  $100 \times 150 \mu\text{m}^2$  pixels, followed by ten microstrip layers with pitches between 80 and 180  $\mu\text{m}$ . The silicon tracker provides the vertex position with  $\sim 15 \mu\text{m}$  accuracy.

Muons are measured in gas chambers embedded in the iron return yoke in the pseudorapidity window  $|\eta| < 2.4$ , with detection planes made of three technologies: Drift Tubes, Cathode Strip Chambers, and Resistive Plate Chambers. Matching the muons to the tracks measured in the silicon tracker results in a transverse momentum resolution between 1 and 5%, for  $p_T$  values from 3 GeV up to 1 TeV.

### 3. THE TRIGGER

The first level (L1) of the CMS trigger system, composed of custom hardware processors, uses coarsely segmented information from the calorimeters and muon detectors, while holding all the high-resolution data in pipeline memories in the front-end electronics. The L1 achieves a reduction from the initial 40 MHz bunch-crossing frequency to an accept rate of 100 kHz with a latency of 3.2  $\mu\text{s}$  [2]. The high-level trigger (HLT) processor farm further decreases the event rate from 100 kHz to approximately 100 Hz before data storage. The rate reduction is achieved with reconstruction techniques similar to those used for offline reconstruction [3].

Only a limited trigger bandwidth is available

for heavy flavour physics at CMS with the bulk dedicated to high transverse momentum physics such as searches for the Higgs boson. Most of the heavy flavour physics programme at CMS is based on a dimuon trigger at L1. The dimuon trigger requires the presence of two muons above a given  $p_T$  value. For the initial running at low luminosity it is foreseen that the dimuon trigger operating with a threshold of 3 GeV on the transverse momentum of the muons will fit within the trigger budget with a rate of 0.9 kHz. The low  $p_T$  threshold for the dimuon trigger allows efficient reconstruction of heavy flavour decays to final states with (at least) 2 muons. For some decays a single muon L1 trigger is also useful. The rate is much higher, so a tighter requirement of  $p_T > 14$  GeV must be made to fit within CMS requirements.

In the HLT,  $B$  candidates are identified with a partial reconstruction of the decay products in the tracker by considering only restricted tracking regions and imposing vertex and invariant mass requirements. A partial track reconstruction algorithm is used to collect only enough information as is needed for tracking. The first 5 or 6 hits typically provide sufficient precision for most HLT applications such as vertex reconstruction and b-tagging [4].

The primary interaction vertex is reconstructed using only hits from the pixel detectors. The partial tracking regions are defined by cones around the muons found in L1. Muon candidates are then combined as oppositely charged pairs and fit for common vertex compatibility. Requirements on the invariant mass of the dimuon pair are applied, if appropriate. The largest source of background comes from prompt  $J/\psi$  production. Dimuon pairs originating from  $B$  hadrons are identified by the flight length of the parent particle resulting in a dimuon vertex that is displaced from the production vertex.

### 4. SEARCH FOR $B_s^0 \rightarrow \mu^+ \mu^-$

The decay modes  $B_{s(d)}^0 \rightarrow \mu^+ \mu^-$  are forbidden at the tree level in the Standard Model (SM) by the GIM mechanism. They can proceed through higher order effective flavour changing neutral

currents as shown in Fig. 1. The internal quark annihilation required within the  $B$  meson further suppresses the decay by  $(f_B/m_B)^2 \approx 2 \times 10^{-3}$  relative to the electroweak penguin  $b \rightarrow s\gamma$  decay. Additionally, a helicity suppression factor pushes the SM branching fractions down to  $\sim 3 \times 10^{-9}$  [5]. The current best limit for the branching fraction for  $B_s^0 \rightarrow \mu^+\mu^-$  is  $< 6 \times 10^{-8}$  at 95% C.L. from the CDF collaboration [6].

While highly suppressed in the SM, many extensions to the SM allow for the branching fractions to be increased, which makes these decays sensitive probes for physics beyond the SM. In particular, in the MSSM the branching fraction for these decays can be enhanced by orders of magnitude, especially at large  $\tan\beta$  [7].

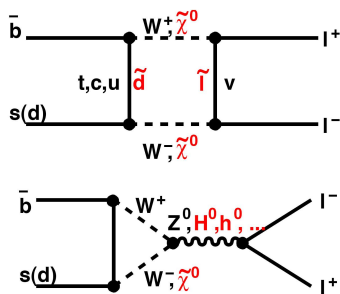


Figure 1. Feynman diagrams for the decays  $B_{s(d)}^0 \rightarrow \mu^+\mu^-$ . In the SM, this decay proceeds through  $W$  and  $Z$  bosons in box (top) and loop (bottom) interactions. In SM extensions new particles can contribute to the processes and increase the branching fractions.

A full Monte Carlo simulation study has been performed to estimate the reach of CMS in the search for the decay  $B_s^0 \rightarrow \mu^+\mu^-$ . Signal and background event samples were generated and passed through a full GEANT-based detector simulation. The muons from signal and QCD multi-jet minimum bias events are required to lie within the detector acceptance [8]. The dominant

background is combinatorial from real muons in the event which fake the signal.

On the trigger level, the dimuon L1 path is used to seed a partial reconstruction in the HLT. Tracks are reconstructed in cones centered on the L1 muon candidate direction until a  $p_T$  precision of 2% is achieved or a maximum of 6 hits are used. All oppositely charged muon pairs are then fit to a common vertex and combinations with a vertex  $\chi^2 < 20$ , an invariant mass within 150 MeV of the  $B_s^0$  mass, and a transverse decay length of at least  $150 \mu\text{m}$  are retained. The  $B_s^0$  mass distribution from the partial reconstruction in the HLT, shown in Fig. 2, has a width of 74 MeV. An estimated 47 signal events remain after the HLT selection for a data sample of  $10 \text{ fb}^{-1}$  [4].

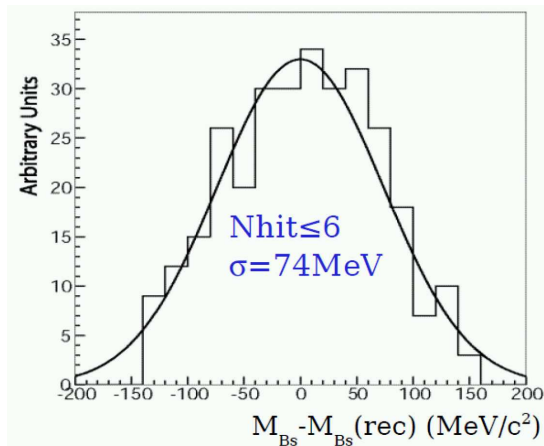


Figure 2. Invariant mass distribution for  $B_s^0 \rightarrow \mu^+\mu^-$  candidates from simulated signal events from a partial reconstruction using at most 6 hits in the high-level trigger.

A full reconstruction is performed in the offline analysis. The two muons must have  $p_T > 4$  and  $|\eta| < 2.4$  and are required to lie within  $0.3 < \Delta R(\mu\mu) < 1.2$  where  $\Delta R(\mu\mu) \equiv \sqrt{\Delta\phi^2 + \Delta\eta^2}$  is the separation of the muon pair in azimuthal angle,  $\phi$ , and pseudorapidity,  $\eta$ . The last re-

quirement helps reject gluon-gluon fusion backgrounds where both  $b$ -hadrons decay semileptonically, which tend to be back-to-back. The dimuon vertex  $\chi^2$  is required to be  $< 1.0$ . The secondary vertex must be displaced from the primary vertex by greater than 18 times its uncertainty in the plane transverse to the beamline.  $B_s^0$  candidate transverse momentum is required to point in the direction of the displacement of the secondary vertex from the primary. The resulting  $B_s^0$  mass resolution is well fit by a double Gaussian with a width of 32 MeV (60 MeV) for the core (tail) component with a weighted-average width of 36 MeV as shown in Fig. 3. The resolution from the offline reconstruction is thus less than half as large as that from the partial reconstruction in the HLT.

The background study is limited by the size of the generated samples, but the uncertainty can be estimated by factorizing the various requirements. In data the background can be estimated by signal sidebands so a limited data sample will not be a problem. The total selection efficiency for signal events is  $(1.9 \pm 0.2)\%$  and the background rejection factor is  $2.7 \times 10^{-7}$ . With this selection, the first  $10 \text{ fb}^{-1}$  will yield a signal of  $6.1 \pm 0.6$  events with a background of  $13.8^{+22.0}_{-13.8}$  events in a window of  $\pm 0.1 \text{ GeV}$  around  $m_{B_s^0}$ . The estimated upper limit on the branching fraction is  $\mathcal{B}(B_s^0 \rightarrow \mu^+\mu^-) \leq 1.4 \times 10^{-8}$  at the 90% C.L.

## 5. THE DECAY $B_s^0 \rightarrow J/\psi\phi$

Many properties of the  $B_s^0$  system, such as the mass and width differences of the two weak eigenstates, can be studied in the decay  $B_s^0 \rightarrow J/\psi\phi$ . Unlike the  $B_d^0$  system, the difference in the widths of the weak eigenstates is large with a relative difference  $\Delta\Gamma_s/\Gamma_s \approx 10\%$  in the SM. Recent measurements from CDF [9] and D0 [10] measure  $\Delta\Gamma_s/\Gamma_s > 10\%$ .

The channel  $B_s^0 \rightarrow J/\psi\phi$  also offers a chance to measure  $CP$  violation in the  $B_s^0$  system. The final state is an admixture of  $CP$ -even and  $CP$ -odd components, which can be resolved by the angular distributions of the final state products. As in  $B^0 \rightarrow J/\psi K_S^0$  in the  $B_d^0$  system, interference can occur between decays that proceed through

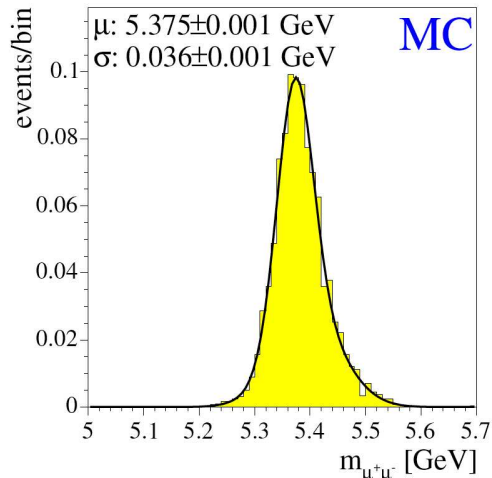


Figure 3. Invariant mass distribution for  $B_s^0 \rightarrow \mu^+\mu^-$  candidates from simulated signal events from full offline reconstruction with all selection requirements applied. The fitted width of 36 MeV is a weighted average of two Gaussian components.

$B^0-\bar{B}^0$  mixing first and those that decay directly to  $J/\psi\phi$ . The weak phase,

$$\phi_{CKM} = [\arg(V_{cs}^*V_{cb}) - \arg(V_{ts}^*V_{tb})], \quad (1)$$

where  $V_{ij}$  represent elements of the CKM quark mixing matrix, can be measured by considering the time-dependent variations of the  $CP$  asymmetry.

The weak phase provides one of the best ways to measure the height of the CKM unitarity triangle,  $\eta$ . To first order in the Wolfenstein parameterization,  $\phi_{CKM} = 2\lambda^2\eta$ , where  $\lambda$  is the  $B_s^0$  mixing parameter. In the SM,  $\phi_{CKM}$  is expected to be small with a value of 0.03, which is beyond current experimental reach. The measurement of a significantly larger weak phase would indicate the presence of new physics. At this time, the flavour tagging tools required to extract the weak phase are not yet available at CMS and only the mixing measurement is considered further here.

The decay  $B_s^0 \rightarrow J/\psi\phi$  is reconstructed through

the decays  $J/\psi \rightarrow \mu^+\mu^-$  and  $\phi \rightarrow K^+K^-$ . The main backgrounds for  $B_s^0 \rightarrow J/\psi\phi$  include prompt  $J/\psi$ , particularly at the trigger lever. For offline reconstruction, inclusive  $b \rightarrow J/\psi X$  decays must be identified. The decay  $B_d^0 \rightarrow J/\psi K^{*0}$  is particularly important to identify because the  $K^{*0}$  decay to  $K^+\pi^-$  can easily be misidentified as  $\phi \rightarrow K^+K^-$ . The  $B_d^0$  decay also has a time-dependent angular asymmetry similar to the  $B_s^0$ , but with different parameters which dilute the measured values if the background is not correctly identified.

The trigger at L1 uses the dimuon selection. The HLT muon selection is the same as described above for  $B_s^0 \rightarrow \mu^+\mu^-$  except the dimuon invariant mass is required to be within 150 MeV of the  $J/\psi$  mass. To reject prompt  $J/\psi$  background, the distance between the dimuon vertex and the primary vertex in the plane transverse to the beam is required to be at least 3 times greater than its uncertainty.

The cosine of the angle between the transverse momentum of the  $J/\psi$  candidate and the direction between the primary vertex and the dimuon vertex in the transverse plane is required to be  $> 0.9$ . With these requirements, 80% of the accepted  $J/\psi$  candidates originate from true  $b$  hadron decays with a trigger accept rate of 15 Hz.

After the  $J/\psi$  selection, a full reconstruction is performed as the final step in the HLT. Cones around the  $J/\psi$  candidates are used to search for charged particle tracks in the tracker. All oppositely charged track pairs are fit to a common vertex with a kaon mass assignment to form  $\phi$  candidates. All pairs with an invariant mass within 20 MeV of the  $\phi$  mass are retained. All four tracks are then fit to a common vertex and candidates with an invariant mass within 200 MeV of the  $B_s^0$  mass are retained. The transverse momenta for the kaon, muon and  $B_s^0$  candidates are required to be greater than 0.7 GeV, 1.0 GeV and 5 GeV, respectively. The final HLT rate is well below 0.1 Hz.

In the offline reconstruction, charged tracks are reconstructed using the full standard tracking reconstruction and combined with signals from the muon chambers to identify muons. Additional muon identification is performed with informa-

tion from the calorimeters combined with the muon chambers. Two oppositely charged muons are combined to form a  $J/\psi$  candidate and two oppositely charged tracks are combined to form a  $\phi$  candidate. Because CMS does not have particle identification appropriate for identifying charged kaons, all track candidates are considered as possible kaon candidates, which adds substantially to the combinatorial background.

A kinematic fit of the four final-state tracks is performed with the invariant mass of the two muons constrained to the  $J/\psi$  mass with the requirement that all four tracks originate from a common vertex. The confidence level of the kinematic fit is required to be greater than  $1 \times 10^{-3}$ . The invariant mass of the two kaon candidates is required to be within 8 MeV of the  $\phi$  mass. Lastly, the cosine of the angle between the reconstructed momentum vector of the  $B_s^0$  candidate and the vector pointing from the production vertex to the decay vertex is required to be larger than 0.95. The final resolution for the  $B_s^0$  meson mass is found to be 14 MeV and is shown in Fig. 4.

With all of the selection requirements described above, a sample of 327 000 signal events is expected in  $30 \text{ fb}^{-1}$  of data with a background of 109 000 events *without* a requirement on the 4-track invariant mass. Such a requirement would significantly reduce the background without substantial loss of signal efficiency. With this data sample, an untagged time-dependent analysis of the  $B_s^0$  candidates can be used to extract the  $B_s^0$  mixing parameters,  $\Delta\Gamma_s$  and  $\Gamma_s$ .

A sample corresponding to an integrated luminosity of  $1.3 \text{ fb}^{-1}$  was generated along with a realistic ratio of  $B_d^0 \rightarrow J/\psi K^{*0}$  events. The background sample after the selection requirements was not large enough to determine the time-dependent angular distributions for  $J/\psi K^{*0}$ . Instead, the selected  $J/\psi K^{*0}$  events were included with the signal events and fit in a time-dependent maximum likelihood fit with a single probability density function for signal. The results of the fit are shown in Table 1. A first measurement of the ratio  $\Delta\Gamma_s/\Gamma_s$  can be made with 20% precision with  $1.3 \text{ fb}^{-1}$  of data. Integrating  $10 \text{ fb}^{-1}$  the statistical uncertainty is estimated to be reduced

Table 1

Results from the maximum likelihood fit for  $B_s^0$  mixing parameters in the decay  $B_s^0 \rightarrow J/\psi\phi$  from simulated signal and background events corresponding to  $1.3 \text{ fb}^{-1}$  of data.

Parameter	Input value	Result	Stat. error	Syst. error
$\bar{\Gamma}_s \text{ (ps}^{-1}\text{)}$	0.712	0.706	0.008	0.023
$\Delta\Gamma_s \text{ (ps}^{-1}\text{)}$	0.142	0.144	0.026	0.011
$\Delta\Gamma_s/\bar{\Gamma}_s$	0.2	0.204	0.037	0.017

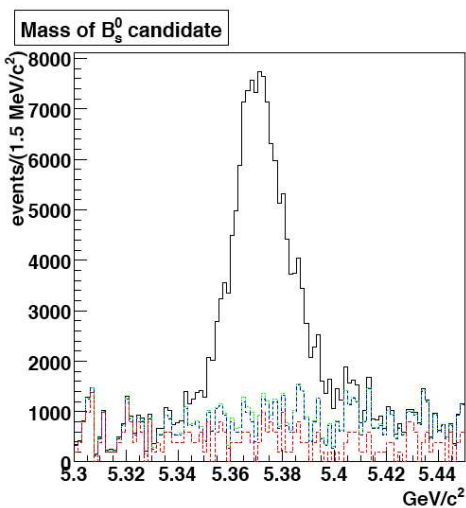


Figure 4. Invariant mass distribution for  $B_s^0 \rightarrow J/\psi\phi$  candidates from simulated signal (solid) and background inclusive  $b \rightarrow J/\psi X$  (dashed line) and  $B^0 \rightarrow J/\psi K^{*0}$  (dashed-dotted) events from full offline reconstruction with all selection requirements applied.

to 0.011 or 5% precision.

Systematic uncertainties are estimated and included in Table 1. The most difficult systematic effect to understand is the time-dependent efficiency function. The requirements in the HLT on the proper decay length significance needed to reject prompt  $J/\psi$  mesons distort the efficiency for reconstructing displaced tracks. Uncertainty on this time-dependent efficiency function is the largest systematic uncertainty in the measure-

ment.

## 6. STUDY OF THE $B_c^+$ MESON

The  $B_c^+$  meson is the ground state of the doubly heavy flavoured  $\bar{b}c$  system. The meson was discovered by the CDF collaboration, with a measured mass of  $6.276 \pm 0.004 \text{ GeV}$  [12], and confirmed by the D0 collaboration, which makes the most precise lifetime measurement of  $0.45 \pm 0.05 \text{ ps}$  [13]. The  $B_c^+$  meson provides an opportunity to study heavy quark dynamics and to test non-relativistic QCD [14] and to study production mechanisms in hadron collisions [15].

The  $B_c^+$  meson is reconstructed in the decay  $B_c^+ \rightarrow J/\psi\pi^+$ , with  $J/\psi$  decaying to 2 muons [16]. The most important backgrounds for the decay arise from prompt  $J/\psi$  production as discussed in Sec. 5 and from other  $B$  decays with a  $J/\psi$  in the final state. A sample of 52 000 simulated signal events that decay within the acceptance of the detector, corresponding to  $30 \text{ fb}^{-1}$  of data, was produced with a full detector simulation. Prompt  $J/\psi$ ,  $B \rightarrow J/\psi X$ ,  $c\bar{c} \rightarrow \mu^+\mu^- X$ ,  $b\bar{b} \rightarrow \mu^+\mu^- X$ , QCD, and  $W$  and  $Z$  boson background events were also generated and passed through the detector simulation.

The trigger selection is similar to that of  $B_s^0 \rightarrow J/\psi\phi$ , with only one hadron track as opposed to two. The final selection applies a vertex fit of the two muons and requires the fitted invariant mass to be within 100 MeV of the  $J/\psi$  mass. A kinematic fit is applied to the three final-state tracks with the dimuon mass constrained to the  $J/\psi$  mass. The transverse flight length of the  $B_c^+$  candidate is required to be greater than 2.5 times its uncertainty and greater than  $60 \mu\text{m}$  to reject prompt  $J/\psi$  candidates. Additionally, the cosine

of the angle between the  $B_c^+$  candidate momentum and its flight length must be greater than 0.8.

These requirements reduce the backgrounds to low levels. The largest background is from  $B \rightarrow J/\psi X$  with an estimated  $2.6 \pm 0.4$  events/fb $^{-1}$  compared with  $120 \pm 11$  events/fb $^{-1}$  for signal. The number of simulated events for the multi-jet QCD background is not sufficient to estimate it with all selection criteria applied at once. A factorized approach is taken to estimate a multi-jet QCD background of  $0.7 \pm 0.1$  events/fb $^{-1}$ . All other backgrounds are at the level of less than 0.1 events/fb $^{-1}$ .

From a sample representing 1 fb $^{-1}$  of data, the mass of the  $B_c^+$  is obtained from the kinematic fit with a result of  $m_{B_c^+} = 6402.0 \pm 2.0$  MeV when the simulated input value was 6400 MeV. The invariant mass spectrum for signal and background is shown in Fig. 5. A binned likelihood fit to the proper decay length distribution is used to extract the  $B_c^+$  lifetime. A fitted value of  $148.8 \pm 13.1$   $\mu$ m was found with an input value of 150  $\mu$ m. From just 1 fb $^{-1}$  of data the  $B_c^+$  mass and lifetime measurements from CMS should be very competitive with the current best values.

## 7. SEARCH FOR $\tau^- \rightarrow \mu^- \mu^- \mu^+$

The decay  $\tau^- \rightarrow \mu^- \mu^- \mu^+$  is forbidden by conservation of lepton number in the SM. Including massive neutrinos in the SM allows for some lepton flavour violation, but predicts a tiny branching fraction for  $\tau^- \rightarrow \mu^- \mu^- \mu^+$ , around  $10^{-30}$ , well below foreseeable experimental reach. However, more sources of LFV and  $\tau^- \rightarrow \mu^- \mu^- \mu^+$  branching fractions of order  $10^{-(7-10)}$  are predicted by a variety of extensions to the SM such as mSUGRA with a branching fraction prediction  $\sim 10^{-9}$  [17]. The current experimental limit, set by the Belle collaboration, is already pushing into the predicted territory with a value of  $< 3.2 \times 10^{-8}$  at 90% C.L. [18].

At the LHC, an estimated  $3 \times 10^{11}$   $\tau$  leptons will be produced for each fb $^{-1}$  of data. The largest sources are from  $B$  and  $D$  meson decays with around  $1.5 \times 10^{11}$ /fb $^{-1}$ . Sources from  $W$  and  $Z$  gauge bosons are reduced by 4 and 5 orders

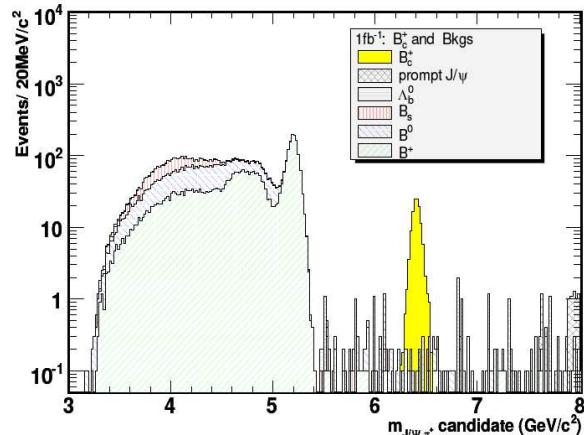


Figure 5. Semi-log plot of the invariant mass distribution for the  $B_c^+$  meson for simulated signal and background events based on 1 fb $^{-1}$  of data.

of magnitude, respectively. While the  $B$  and  $D$  sources are much more plentiful, the muon momenta are low and the L1 dimuon  $p_T > 3$  GeV requirement offsets the 4 to 5 orders of magnitude gained by the cross sections. Alternatively, the muons from  $\tau^- \rightarrow \mu^- \mu^- \mu^+$  decays from  $\tau$  leptons produced from  $W$  and  $Z$  sources are much more energetic and are retained by the trigger with high efficiency.

A simulation study at CMS considered the possible reach for  $\tau^- \rightarrow \mu^- \mu^- \mu^+$  reconstruction from three sources:  $B$  mesons,  $W$  bosons, and  $Z$  bosons. The  $W^- \rightarrow \tau^- \nu_\tau$  boson source showed the greatest sensitivity and is described below [19].

A total efficiency for the trigger of 62% can be achieved by selecting events with a single muon with  $p_T > 19$  GeV and events with two muons, each with  $p_T > 7$  GeV. In offline reconstruction, the three muons are combined with a vertex fit and retained if the invariant mass is within 25 MeV of the  $\tau$  mass. An observed missing  $E_T$  of at least 20 GeV is also required from the unobserved neutrino. After the selection, the largest background remaining arises from the de-

cay  $D_s \rightarrow \mu\nu\phi(\mu\mu)$  which has exactly the same final state as the signal. A veto is applied for any pair of oppositely charged muons that have an invariant mass consistent with the  $\phi$  meson. A kinematic fit to simulated signal events finds a  $\tau$  invariant mass distribution with a width of 24 MeV.

With the selection requirements above, a sensitivity of  $7.0(3.8) \times 10^{-8}$  with  $10(30) \text{ fb}^{-1}$  of data at 95% C.L. can be reached. The  $Z$  boson and  $B$  meson  $\tau$  sources are found to have an expected reach of 3.4 and  $2.1 \times 10^{-7}$  at 95% C.L. with  $30 \text{ fb}^{-1}$ . The results from each of the three channels can be combined for a final result more sensitive than the individual channels. Unlike the previously described  $B$  decay reconstructions, this analysis does not rely on extremely low  $p_T$  muons to pass the L1 and will be sensitive beyond the initial low luminosity running period.

## 8. CONCLUSIONS

The CMS detector is well suited for a variety of heavy flavour physics measurements. The outstanding all-silicon tracking system will provide excellent momentum resolution and vertex displacement precision in the very dense tracking environment of the LHC. The powerful muon system allows for a low  $p_T$  dimuon level-1 trigger to collect the relevant data samples during the initial low luminosity running period. Searches for new physics in branching fractions and asymmetries and the study of properties of rare particles are possible in a variety of channels with the large data sample that will be provided by the LHC and collected by the CMS detector.

## REFERENCES

1. S. Chatrchyan *et al.* [CMS Collaboration], JINST **3** S08004, 2008.
2. CMS Collaboration, CERN/LHCC 2002-26, CMS TDR 006-1, 2000.
3. CMS Collaboration, CERN/LHCC 2000-38, CMS TDR 006-2, 2002.
4. CMS Collaboration, CERN/LHCC 2006-001, CMS TDR 008-1, 2006.
5. A. J. Buras, Phys. Lett. B **566**, 115 (2003).
6. T. Aaltonen *et al.* [CDF Collaboration], Phys. Rev. Lett. **100**, 101802 (2008).
7. K. S. Babu and C. F. Kolda, Phys. Rev. Lett. **84**, 228 (2000).
8. U. Langenegger [CMS Collaboration], arXiv:hep-ex/0610039v2.
9. T. Aaltonen *et al.* [CDF collaboration], Phys. Rev. Lett. **100**, 121803 (2008).
10. V. M. Abazov *et al.* [D0 Collaboration], arXiv:0802.2255 [hep-ex].
11. V. Ciulli *et al.* [CMS Collaboration], CMS NOTE-2006/090.
12. T. Aaltonen *et al.* [CDF collaboration], Phys. Rev. Lett. **100**, 182002 (2008).
13. V. M. Abazov *et al.* [D0 Collaboration], arXiv:0805.2614 [hep-ex].
14. X. G. Wu *et al.* Phys. Rev. D **67**, 094001 (2003).
15. C. H. Chang *et al.* Eur. Phys. J. C **38**, 267 (2004).
16. X. W. Meng *et al.* [CMS Collaboration], CMS NOTE-2006/118.
17. J. R. Ellis *et al.* Phys. Rev. D **66**, 115013 (2002).
18. Y. Miyazaki *et al.* [Belle Collaboration], arXiv:0711.2189 [hep-ex].
19. R. Santinelli *et al.* [CMS collaboration], CMS NOTE-2002/037.